GENERATION AND STABILITY OF INTENSE LONG FLAT BUNCHES

F. Zimmermann and Ibon Santiago Gonzalez*, CERN, Geneva, Switzerland

Abstract

This report surveys possible schemes for producing long, "flat", intense bunches of about 5×10^{11} protons spaced by 50 ns, as are required by one of the proposed LHC upgrade scenarios. It also examines potential intensity limitations and instability thresholds for such beams.

THE ISSUE

The "large Piwinski angle" (LPA) scenario of the LHC upgrade [1] requires bunches of 5×10^{11} protons, spaced by 50 ns, with a flat longitudinal profile.

For demonstrating the feasibility of such upgrade path, the following questions must be addressed:

- How and where can such intense bunches be generated?
- How and where can they be made flat?
- Do these bunches remain stable and do they preserve their longitudinally flat shape?

This paper attempts to take a first look at the above questions.

GENERATION OF INTENSE BUNCHES

For the LPA scheme we should produce bunches of about 5×10^{11} protons at 50 ns spacing in the LHC. The Superconducting Proton Linac (SPL) and the PS2 are being designed to deliver 4×10^{11} protons per bunch at 25 ns spacing, which corresponds to the expected space charge limit at PS2 injection. Therefore, generating an intensity of 4×10^{11} protons per bunch at 50 ns spacing is easy with SPL and PS2, by injecting only every second bunch from the linac into the PS2. The higher bunch intensity $\sim 5.5 \times 10^{11}$ needed for LPE (with some margin for downstream losses) may be reached by one of the following methods:

- raising the SPL energy by about 17%;
- bunch merging at PS2 extraction;
- slip stacking in the SPS; or
- slip stacking in the LHC.

Raising the SPL energy would have implications on the linac length or linac gradient required. Bunch merging or slip stacking could result in increased beam losses and activation problems. Depending on where these longitudinal bunch manipulations are performed, additional RF systems will be required in the PS2, the SPS or the LHC itself.

* On leave from University of the Basque Country, Bilbao, Spain

STABILITY OF INTENSE BUNCHES

In the SPS intensity limits for LPA arise from the Transverse Mode Coupling Instability (TMCI) and from a longitudinal coupled bunch instability, while electron cloud is not expected to be a problem at 50-ns bunch spacing [1].

The effective transverse SPS single-bunch broad-band impedance $|Z_y^{BB}|$ for a 0.5 rms bunch length has been about 23 MΩ/m in 2006 and 2007. This value was inferred from the measured vertical tune shift (see Fig. 1) and head-tail growth rate as a function of intensity or chromaticity, respectively [2, 3]. The measurement uncertainty is 10-20%. Changes from one year to the next of up to 30% were found to well track the removal or addition of high-impedance components, e.g. kicker magnets, and to be close to expectation [2, 3].

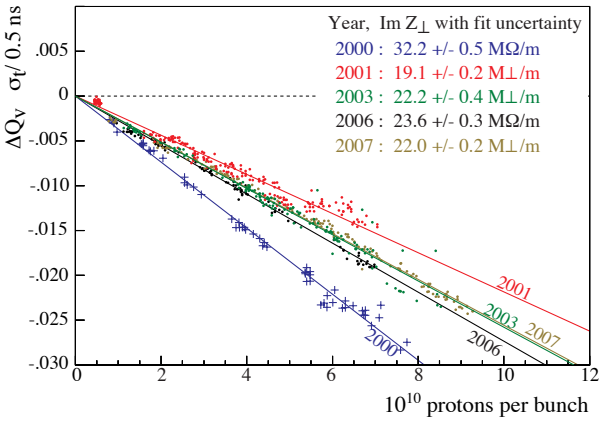

Figure 1: Vertical betatron tune as a function of intensity measured at the SPS in various years [3].

The Transverse Mode Coupling Instability is observed with a proton beam at the SPS [4, 5]. The measured threshold intensity is well described by the theoretical expression [4]

$$N_{b,thr} \approx \frac{8\pi Q_y \epsilon_{||}}{e^2 c} \frac{f_{rev}}{|Z_y^{BB}|} \left(1 + \frac{f_\xi}{f_r}\right) , \qquad (1)$$

Where $\epsilon_{||}$ denotes the longitudinal rms emittance, Q_y the betatron tune, e the electron charge, c the speed of light, f_r the effective broadband resonator frequency, $\eta \equiv (1/\gamma^2 - \alpha_C)$ the slippage factor, and $f_\xi = Q'\omega_0/\eta$ the chromatic

frequency shift (where ω_0 denotes the angular revolution frequency).

With the present typical longitudinal emittance of $\epsilon_{||} \approx 0.2$ eVs, Eq. (1) predicts the TMCI threshold for $N_{b,thr} \approx 10^{11}$ protons at a beam energy of 26 GeV, which is consistent with the experimental results, but about a factor 2 higher than the threshold simulated by the code HEADTAIL [5] without space charge, as is illustrated in Fig. 2. The difference between observed and simulated thresholds decreases if space-charge effects are included in the simulation [6].

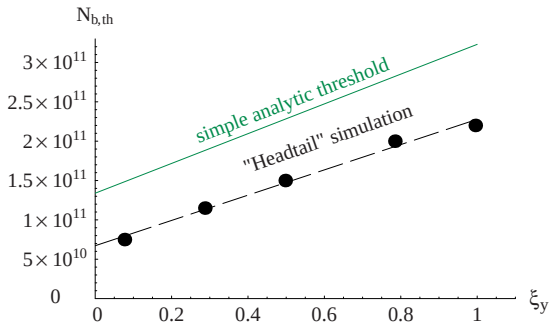

Figure 2: Instability thresholds according to Eq. (1) and from simulations with the code HEADTAIL as a function of vertical chromaticity [5].

In view of the reasonable consistency with the experiments, we can apply (1) to extrapolate the threshold that we should expect for intense bunches in the PS2. Tripling the longitudinal emittance will increase the threshold three times. Raising the injection energy from 26 GeV in the present SPS to 50 GeV for injection from a PS2, will increase the magnitude of the slippage factor, $|\eta|$ by a factor 2.5, and, finally, operating with a chromaticity of $Q' \approx 10$ will give another factor of 2. Putting everything together, we expect that the TMCI threshold in the SPS can easily be shifted towards 1.5×10^{12}, far above our target value of 5.5×10^{11} protons per bunch.

A concern related to TMCI will arise, however, if we decide to flatten the bunches by means of a higher harmonic RF system, since the TMCI threshold may go to zero in such a case [7].

The longitudinal broadband impedance of the SPS is estimated from the measured shift of the quadrupole oscillation frequency with bunch intensity [9]. In 2007 a value $Z/n \approx 10\ \Omega$ was obtained [8], as is illustrated in Fig. 3. The longitudinal broadband impedance can lead to a loss of Landau damping against coupled-bunch instabilities. Figure 4 shows how the threshold for coupled-bunch instabilities decreases with increasing beam energy in the SPS. Without the stabilizing third harmonic 800-MHz system the threshold at top energy is only $N_{b,thr} \approx 2 \times 10^{10}$ ($N_{b,thr} \approx 1.3 \times 10^{11}$ at injection). With the 800 MHz system turned on in "bunch shortening mode" the instability occurs only on the SPS flat top, up to nominal intensities ($N_b \approx 1.2 \times 10^{11}$) [9]. The beam can be further stabilized by a controlled blow up of the longitudinal emittance, since the threshold increases roughly in proportion to $\epsilon_{||}^2$ [9].

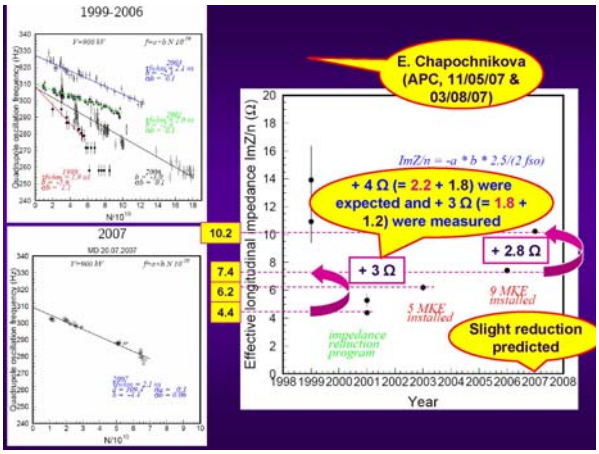

Figure 3: Quadrupole oscillation frequency in the SPS as a function of intensity in various years (left) and the inferred effective longitudinal impedance Z/n versus the year (right) (E. Metral, E. Shaposhnikova et al.) [8].

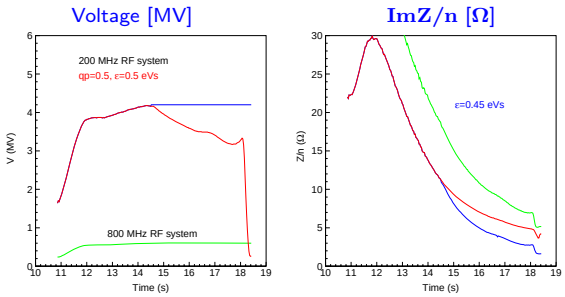

Figure 4: RF voltage programmes for the 200-MHz and 800-MHz systems as a function of time during the SPS cycle (left) and the corresponding longitudinal instability thresholds (right) (E. Shaposhnikova) [8].

HOW TO MAKE "FLAT" BUNCHES?

This question was already studied in depth by J.-P. Delahaye and co-workers in 1980 [10], who distinguished two basic approaches: (1) a modification of the beam distribution, or (2) a change of potential.

Either in the LHC itself or in its injector complex several techniques are available:

- 2nd harmonic debuncher in the linac (J.-P. Delahaye et al, 1980 [10], Fig. 5);
- empty bucket deposition in debunched beam (J.-P. Delahaye et al 1980 [10], A. Blas et al, 2000 [11], Fig. 6);

- higher harmonic cavity (J.-P.Delahaye et al, 1980 [10], Fig. 7);
- blow up by modulation near f_s together with a higher frequency RF near the harmonic frequency (R. Garoby, S. Hancock, 1994 [12], Fig. 8);
- the recombination with an empty bucket using a double harmonic RF system (C. Carli, M. Chanel, 2001 [13, 14], Fig. 9);
- the redistribution of phase space using a double harmonic RF system (C. Carli, M. Chanel, 2001 [13, 14], Figs. 10 and 11);
- RF phase jump (RHIC [15], Fig. 12)
- injection of band-limited noise (E. Shaposhnikova).

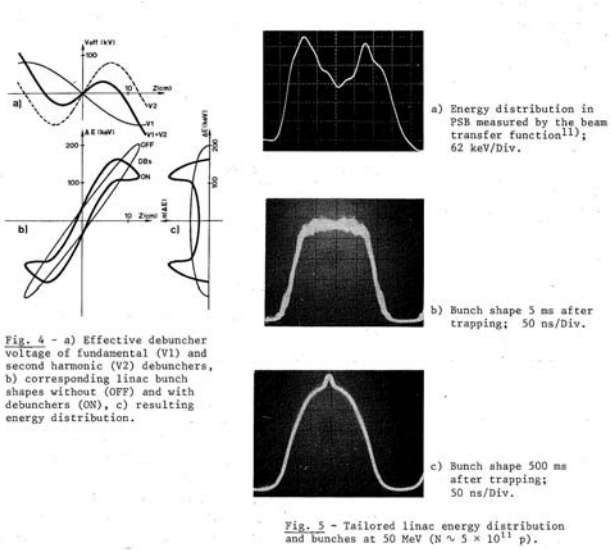

Fig. 4 - a) Effective debuncher voltage of fundamental (V1) and second harmonic (V2) debunchers, b) corresponding linac bunch shapes without (OFF) and with debunchers (ON), c) resulting energy distribution.

Fig. 5 - Tailored linac energy distribution and bunches at 50 MeV (N ∿ 5 × 10^{11} p).

Figure 5: Example for bunch flattening by second harmonic linac debuncher (J.-P. Delahaye et al, 1980 [10]).

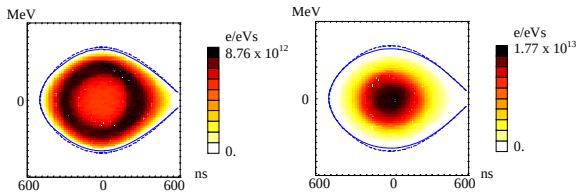

To the left, a flat bunch of 7.4×10^{12} protons and, to the right, a normal bunch of the same intensity. Note the different density scales.

Figure 6: Example for bunch flattening by empty bucket deposition (A. Blas et al, 2000 [11]).

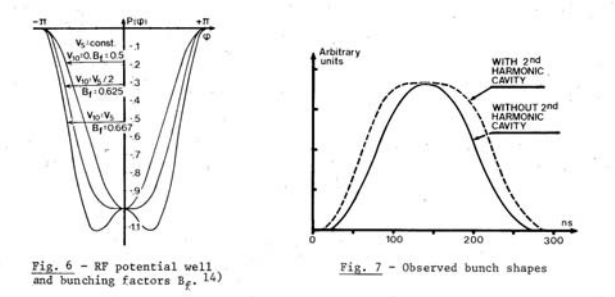

Fig. 6 - RF potential well and bunching factors B_f. [14]

Fig. 7 - Observed bunch shapes

Table 4 - Typical intensities per pulse accelerated in ring 3 (in units of 10^{12} p).

RF voltage	Injection (50 MeV)	After capture	At 200 MeV
Fundamental (V_5) only	9.6	6.3	5.9
2nd-harmonic (V_{10}) added (V_{10} = 0.5 V_5)	9.8	7.8	7.2

Figure 7: Example for bunch flattening by second harmonic ring cavity (J.-P. Delahaye et al 1980 [10]).

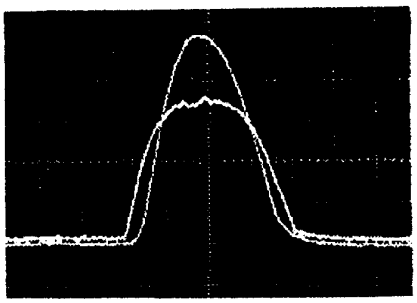

50 ns/div.

Figure 8: Example for bunch flattening by blow up via modulation near f_s together with higher harmonic RF (S. Garoby, S. Hancock, 1994 [12]).

ARE “FLAT” BUNCHES STABLE?

We look at four different aspects of this problem:

- Landau damping for a double RF system;
- Landau damping for a flat bunch in a single RF system;
- stability of hollow bunches with RF & phase loop; and
- the effect of intrabeam scattering.

Landau Damping for a Double RF System

By a double harmonic RF system the bunches can be either lengthened or shortened, depending on the relative phase of the higher harmonic RF wave with respect to the fundamental RF wave. The bunch lengthening mode would also lead to flatter bunches. Therefore this would be the ideal operation mode for our purpose of producing long flat bunches at the LHC. However, there is a problem, pointed out by E. Shaposhnikova [9, 16, 17]. Namely in the bunch

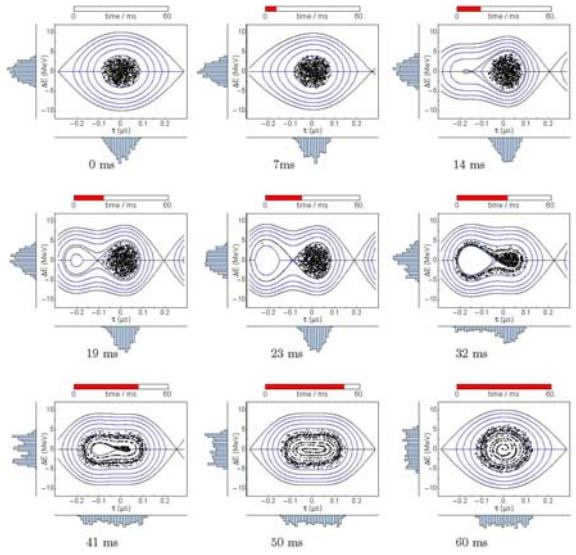

Figure 4: *Blow-up by recombination of a bunch with an empty bucket with improved adiabaticity at small amplitudes. Simulated phase space portraits at different times during the process, with RF parameters versus time plotted in Figure 3.*

Figure 9: Simulation example for bunch flattening by recombination with an empty bucket: empty phase space is inserted close to the bucket center (C. Carli, M. Chanel, 2001 [13, 14]).

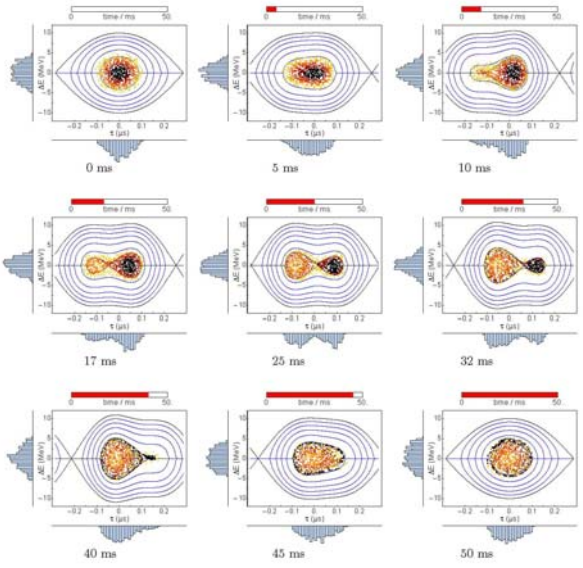

Figure 6: *Redistribution of phase space surfaces to create hollow bunches. Simulated phase space portraits at different times during the process, with RF parameters versus time plotted in Figure 5.*

Figure 10: Simulation example for bunch flattening by redistribution of phase-space surfaces: high-density region and periphery are exchanged (C. Carli, M. Chanel, 2001 [13, 14]).

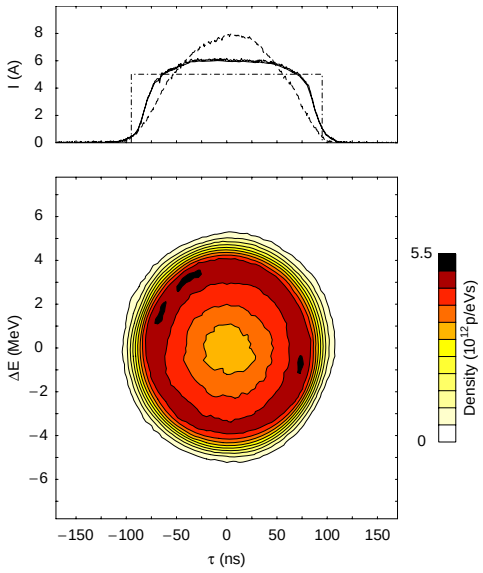

Figure 11: Example for bunch flattening by redistribution of phase-space surfaces: measurement with 6×10^{12} protons per bunch in the PS Booster (C. Carli, M. Chanel, 2001 [13, 14]).

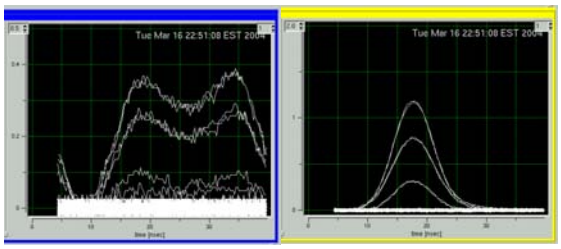

Figure 12: Example for bunch flattening by RF phase jump in RHIC: gold beam, store at 100 GeV/u with h=360 RF system; no collision, no Landau cavity, no dampers, no kickers; hollow beam in the RHIC blue ring, created by RF phase jump, compared with a normal beam in the yellow ring (J. Wei et al [15]).

lengthening mode a critical value of the longitudinal emittance exists above which the bunches do no longer self-stabilize. This critical value is related to the longitudinal oscillation amplitude (or action I) at which the synchrotron tune assumes its maximum value, or $\omega'(I) = 0$, and where Landau damping is lost. Figure 13 compares the variation of the synchrotron tune with amplitude for a single RF system with the one for a double RF in either bunch lengthening or bunch shortening mode. A pronounced maximum of the synchrotron tune at an intermediate amplitude is found only for the bunch lengthening configuration. This extremum inside the beam distribution lies at the origin of the latent beam instability for this case.

Indeed, at the CERN SPS large coherent signals were

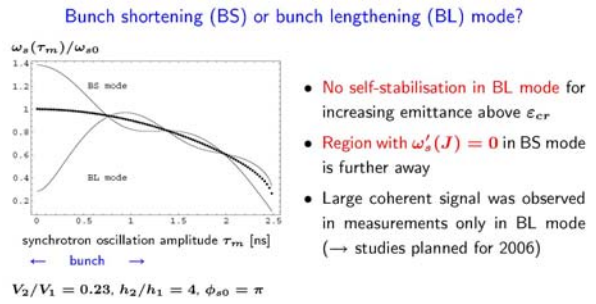

Figure 13: The SPS synchrotron tune as a function of longitudinal oscillation amplitude for a single RF system and for a double RF system in bunch shortening (BS) or bunch lengthening mode (BL); the synchrotron tune is normalized to the central tune for the single RF system. The voltage ration of double harmonic or single harmonic RF is 0.23. The second RF system operates at 4 times the base frequency (800 and 200 MHz, respectively) [9].

observed in beam measurements only when the double harmonic RF was active in bunch lengthening mode. The loss of Landau damping for this 'bad' phasing of the higher harmonic RF is also evidenced by SPS beam-transfer function measurements, illustrated in Fig. 14. Figure 15, also from the SPS, presents detailed images of the bunch shape evolution with a double RF system, which reveal the creation of shoulders in regions where the distribution function F_0 has zero derivative, $dF_0/dJ = 0$, corresponding to the regions with maximum synchrotron tune.

The HEADTAIL programme [18] was recently upgraded by G. Rumolo, in order to model the SPS situation with a double RF system [19]. A higher order harmonic cavity element has become available, which can be switched on and ramped. The extended code was tested for present SPS parameters with a combination of 200-MHz and 800-MHz cavities. The HEADTAIL simulations can now predict the SPS bunch shapes for a double RF system operated in either bunch lengthening or bunch shortening mode. Preliminary results are displayed in Fig. 16.

Landau Damping for Flat Bunches and Single RF

Flat distributions can be obtained from the Ruggiero-Berg class of generalized parabolic distributions [20]

$$\lambda(z) = \frac{n(n+1)\Gamma(n)}{\hat{\tau}\sqrt{\pi}\Gamma(n+\frac{3}{2})}\left(1+\frac{r^2}{\hat{\tau}^2}\right)^{n+\frac{1}{2}} \quad \text{for } 0 < z < \hat{\tau}\ , \tag{2}$$

by taking the limit $n =\!\!\rightarrow -1/2$, where r denotes the radial coordinate in longitudinal phase space. Examples of this and various other Berg-Ruggiero parabolic-like distributions as well as an alternative better behaved flat distribution à la Furman [21] (including its Abel transform [22]) are illustrated in Fig. 17, both as (projected) longitudinal density in physical space and as radial density in

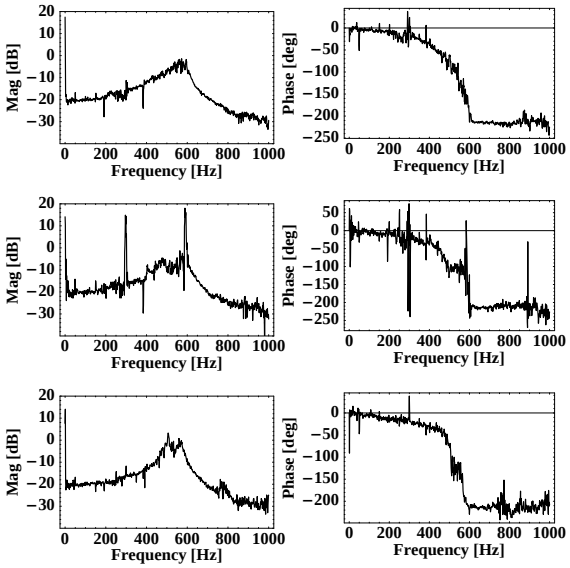

Figure 14: Longitudinal amplitude (left) and phase response (right) of the CERN SPS beam as a function of excitation frequency for a single RF system (top), for a double RF system in bunch lengthening mode (center) and for a double RF system in bunch shortening mode (bottom); the beam transfer function measurement for the bunch lengthening mode shows a strong coherent response at an excitation frequency corresponding to the synchrotron-oscillation amplitude at which $\omega_s'(I) = 0$ [9, 16].

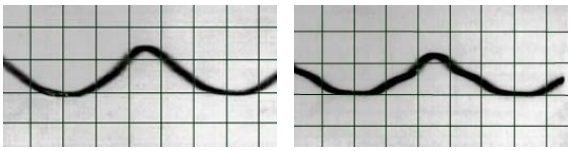

Figure 15: Bunch profiles at the beginning (left) and end (right) of a 10 min. SPS coast at 120 GeV/c in bunch lengthening mode, revealing the development of shoulders [16].

phase space [23]. The calculation in [23] extended earlier Landau-damping considerations of Refs. [24, 25, 26] to longitudinally flat beams.

From the phase-space density the Landau-damping stability limit in the complex tune-shift plane can be calculated using Sacherer's dispersion relation [23, 24]. Examples for elliptical and flat distributions in the Ruggiero-Berg parametrization are displayed in Fig. 18. The direction relevant for finding the tune-shift threshold with space charge below transition (e.g. for the PS) or with an inductive impedance above transition (e.g. for the SPC or LHC) is towards the right. Table 1 summarizes the coherent tune shift stability limits for various different distributions. This table and Fig. 18 demonstrate that flat bunches in a single

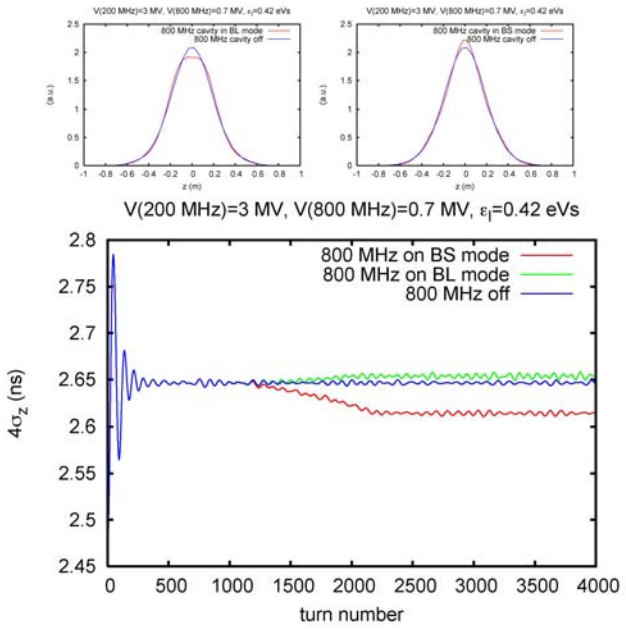

Figure 16: HEADTAIL simulation results for the SPS. The bunch shape with an 800-MHz 3rd harmonic system in bunch lengthening mode compared with the Gaussian shape of a single harmonic RF (top left); the same for the bunch shortening mode (top right); and the 4σ bunch length as a function of turn number for a single RF system and a double RF system in either one of the two operation modes [19].

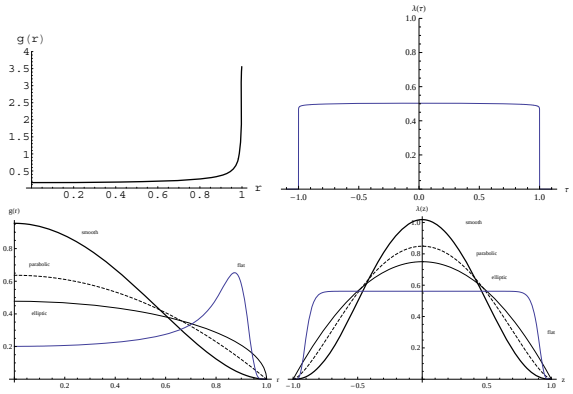

Figure 17: Radial phase space density (left) and longitudinal profile (right) for a flat distribution as limiting case of Ruggiero-Berg class of parabolic distributions (top) as well as for various other quasi-parabolic disttribution functions and another smoother flat distribution à la M. Furman (bottom) [23].

RF system are more stable than any of the considered types of non-flat bunches.

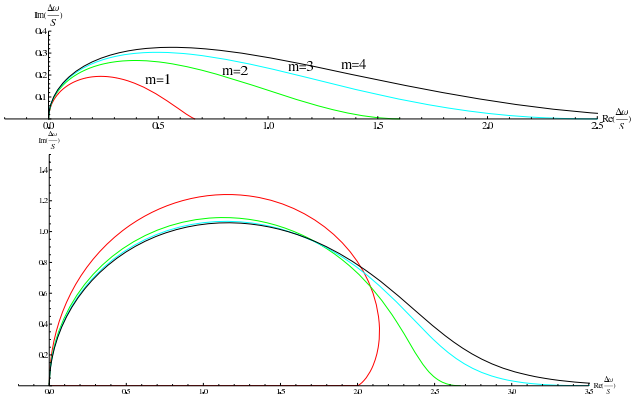

Figure 18: Stability diagrams computed from the Sacherer dispersion relation [24, 23] in the complex tune shift plane, normalized to the bunch synchrotron frequency spread S, for an elliptical distribution with $n = 1/2$ (top) and a flat distribution with $n = -1/2$ (bottom), considering dipole $m = 1$), quadrupolar ($m = 2$) and higher order modes of oscillation [23].

Table 1: Coherent tune shift stability thresholds of the lowest four modes for various longitudinal distributions normalized to the total synchrotron-frequency spread S [23]; $m = 1$ refers to the dipole mode, $m = 2$ to the quadrupolar one, etc.

distribution	n	$\frac{\Delta\omega_1}{S}$	$\frac{\Delta\omega_2}{S}$	$\frac{\Delta\omega_3}{S}$	$\frac{\Delta\omega_4}{S}$
smooth	2	0.33	1	1.8	2.67
parabolic	1	0.5	0.33	2.25	3.2
elliptic	1/2	0.67	1.6	2.57	3.56
flat	$-1/2$	2	2.67	3.6	4.57
flat (Furman)	N/A	1.58	2.13	2.90	3.71

Flat Bunches with Single RF and Phase Loop

Flat or hollow bunches stored in a ring with a single RF can become unstable if an RF phase loop is active [11]. Some pertinent observations from the PS Booster [11] are shown in Fig. 19.

The stability of regular and hollow bunches in single RF systems with RF phase loop was studied by A. Blas, S. Koscielniak et al [11, 27]. These authors considered several typical distributions shown in Fig. 20 (top) and calculated the corresponding Nyquist-Bode stability diagrams of the longitudinal beam-transfer functions (BTF) including phase loop (bottom pictures in Fig. 20). The reference points for the BTF are defined in Fig. 21. An ordinary BTF shows 0 phase lag in the limit of low frequency and a -180 degree shift at high frequencies, passing through -90 de-

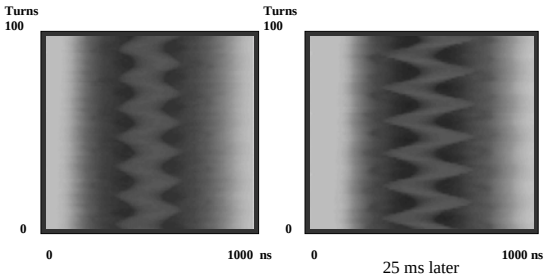

Figure 19: Unstable hollow bunches observed in the CERN PS with both a single RF and active phase loop. The right picture was taken 25 ms after the left [11].

gree between these two extremes. For hollow bunches the derivative of the distribution function is positive for small amplitudes. An additional -90 degree phase change arises from the residue term of the dispersion integral [27]. For significantly hollow bunches, there is a further -90 degree phase change (yielding a total of -360 degree) which is contributed by the principal value of the dispersion integral [27]. A simple interpretation of these findings is that the hollow bunch represents the sum of a positive and a (smaller) negative bunch. The BTF of the negative bunch is simply -1 times that of a positive bunch, and so it has a phase response of $+180$ degree at low frequency and $+0$ degree at high frequency. The phase response of the sum can either lag or lead the excitation. S. Koscielniak concluded that some hollow beams must become unstable when the phase loop is closed; however, the stability and growth rate depend on the degree of hollowness. Figures 22 and 23 illustrate the transition of the BTF from a stable "flat" bunch to an unstable significantly "hollow" bunch.

Longitudinal Emittance Blow Up

In various stages in the LHC accelerator chain (PS Booster, SPS, LHC) the longitudinal emittance is blown up to increase Landau damping and to stabilize the beam. For example, at injection (450 GeV) into the LHC the longitudinal emittance is $0.6-1.0$ eVs. This emittance is blown up during the ramp to reach a value of 2.5 eVs at 7 TeV [28]. In the SPS, the longitudinal emittance of the injected beam at 26 GeV amounts to 0.35 eVs, and it is increased to 0.6 eVs at 450 GeV [29]. All longitudinal emittance numbers here are defined as 4π times the rms energy spread time the rms bunch length, as is customary in the CERN RF group.

It is important to note that the longitudinal blow up during the acceleration of the SPS and the LHC could render useless any prior bunch shaping. Against this background, future more elaborate studies are likely to conclude that the bunch flattening should best be performed in the LHC itself, and ideally at top energy or as part of the longitudinal blow up.

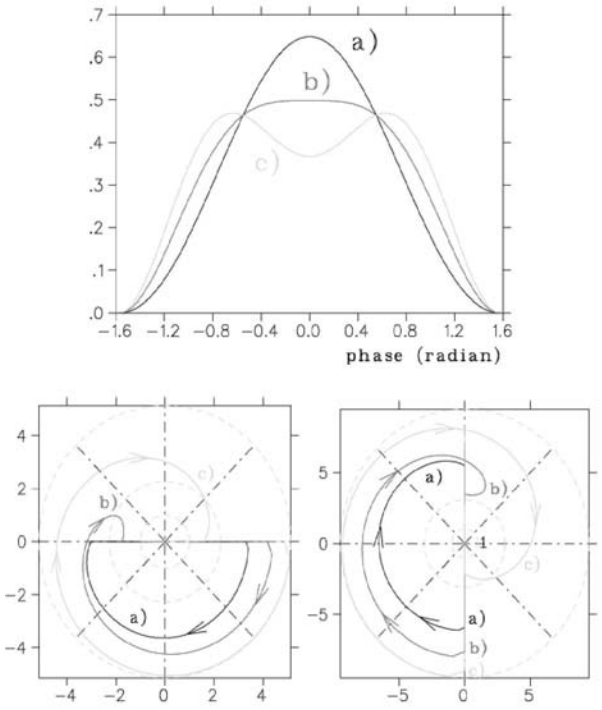

Figure 20: Three different longitudinal distributions for which the stability with RF phase loop was studied (top), and the Nyquist-Bode diagrams of the beam-transfer functions for the same three distributions (bottom). The left picture corresponds to point "1)", the right picture to point "2)" of the phase-loop diagram in Fig. 21. In case of the hollow distribution c the path in the polar diagram surrounds the point $+1$ once in a clockwise sense which indicates instability, while a beam with the flat distribution b is still stable. [11].

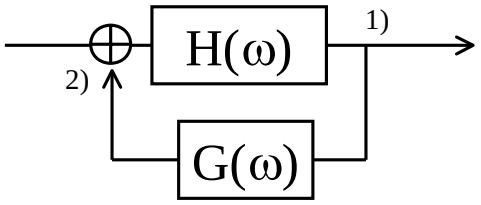

Figure 21: Transfer function diagram in frequency domain for the definition of points "1)" and "2)" used in Fig. 20; $H(\omega)$ denotes the open-loop beam transfer function, and $G(\omega)$ is the phase loop.

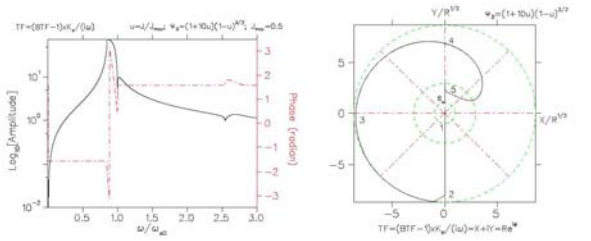

Figure 12: Amplitude/phase and polar plots of the transfer function with phase loop for $\Psi_0 \propto (0.1 + J)(\hat{J} - J)^{3/2}$. The gain $K_p = 3\Omega_s$ per radian.

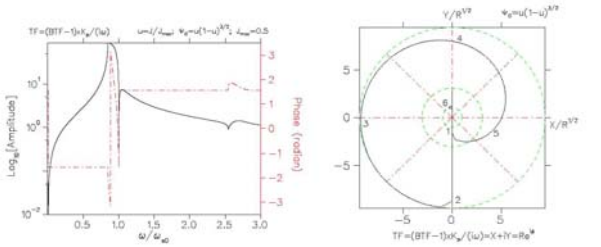

Figure 13: Amplitude/phase and polar plots of the transfer function with phase loop for $\Psi_0 \propto J(\hat{J} - J)^{3/2}$. The gain $K_p = 3\Omega_s$ per radian.

Figure 22: Beam transfer functions in amplitude-phase (left) and Nyquist-Bode representation (right) of a slightly hollow stable bunch (top) and of a significantly hollow unstable bunch (bottom) [27].

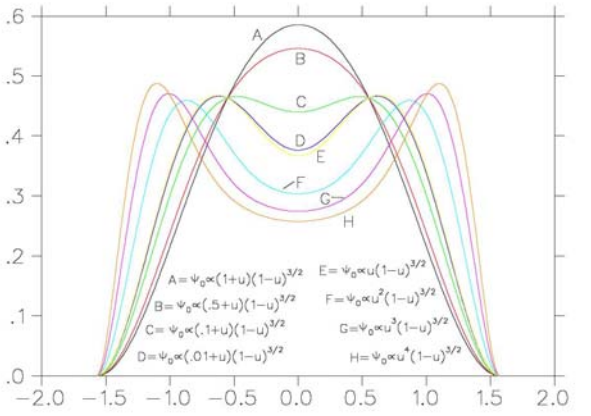

Figure 1: Bunch shapes arising from various phase space distribution functions Ψ_0.

Figure 23: Bunch shapes arising from various phase distribution functions Ψ_0 as indicated; the distribution C is stable while D and E are unstable [27].

Intrabeam Scattering for Flat or Hollow Bunches

We finally address the question whether intrabeam scattering (IBS) could destroy the flat or hollow profile. Machine experiments at, and simulations for, RHIC provide a first tentative answer, noting that IBS is a much stronger effect in RHIC than in the LHC. Figure 24 compares the time evolution of the longitudinal profile for a normal and a hollow beam, as observed in a dedicated RHIC experiment. The former retained its Gaussian-like shape, with increasing rms size, while, after 30 minutes, the hollow beam profile showed a reduction in the depth of its central hole, but was still "flat". Simulations of the profile evolution due to IBS conducted with the code BBFP ("Bunched Beam Fokker-Planck Solver" [31]) are in good agreement with the experimental observations; see Fig. 25 [30]. The IBS calculation in BBFP is performed in action variables. Figure 26 illustrates the calculated time evolution of the density in the longitudinal action space for both hollow and Gaussian beam profiles in RHIC over an interval of 1 h. The BBFP results in terms of action are easily converted to the longitudinal phase and momentum planes.

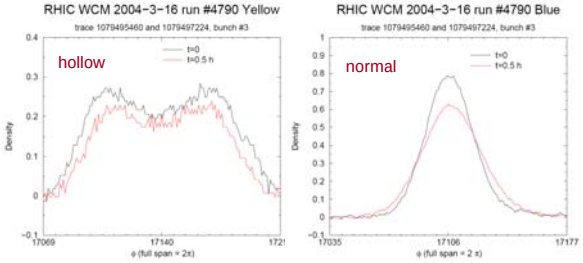

Figure 24: Beam profile evolution for a hollow beam (left) and for a normal beam (right) observed in RHIC; the two curves correspond to the initial profile and to the profile measured after 30 minutes (in red), respectively [30].

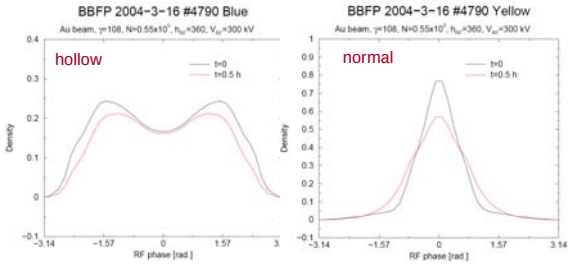

Figure 25: Beam profile evolution for a hollow beam (left) and for a normal beam (right) due to IBS simulated for the beam parameters of the RHIC experiment in Fig. 24; the two curves again correspond to the initial profile and to the profile measured after 30 minutes (in red), respectively [30].

CONCLUSIONS AND OUTLOOK

A concrete scheme for generating the 50-ns LPA beam of an LHC upgrade is still being called for. Several bunch flattening techniques are available and could be applied in various CERN machines. Flat bunches in a single RF system are strongly Landau damped. A double RF system may, however, lead to the loss of Landau damping if the beam distribution extends to the region where $\omega_s(I) = 0$. The ensuing loss of Landau damping is accompanied by the

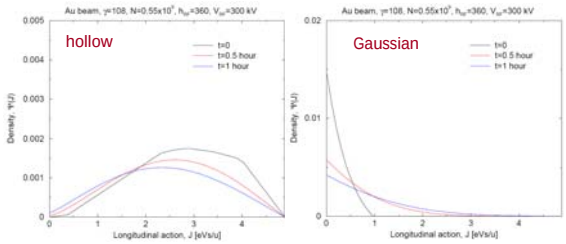

Figure 26: Density evolution in terms of longitudinal action for a hollow beam (left) and for a normal beam (right) due to IBS in RHIC over an interval of 1 h [30].

formation of "shoulders" in the longitudinal profile and by coherent signals. Significantly flat, or hollow, bunches can also become unstable in a single RF system in the presence of an RF phase loop.

The next steps will include (1) further machine studies on beam stability and lifetime in a double RF system, (2) machine studies on flat bunch stability and beam evolution in a single RF system, (3) machine studies on flat-bunch generation, (4) continued analytical studies of Landau damping; (5) simulations with the HEADTAIL and BBFP codes; (6) the development of a detailed strategy to generate intense long flat 50-ns bunches in LHC [in which machine, and by which method(s)?], and (7) the implications for the RF systems in one or several of the upgraded CERN accelerators.

ACKNOWLEDGMENTS

We warmly thank Michael Benedikt, Christian Carli, Steven Hancock, Elias Metral, Yannis Papaphilippou, Giovanni Rumolo, Elena Shaposhnikova, and Jie Wei for helpful discussions. The support of the European Community-Research Infrastructure Initiative under the FP6 "Structuring the European Research Area" programme (CARE, contract number RII3-CT-2003-506395) is gratefully acknowledged.

REFERENCES

[1] F. Zimmermann, "LHC Upgrade Scenarios," PAC2007, Albuquerque (2007).

[2] H. Burkhardt, G. Rumolo, F. Zimmermann, "Coherent Beam Oscillations and Transverse Impedance in the SPS," EPAC 2002 Paris (2002).

[3] H. Burkhardt, "SPS Transverse Impedance Measurements," CERN APC 17.08.2007.

[4] E. Metral, "Stability Criteria for High-Intensity Single-Bunch Beams in Synchrotrons," EPAC 2002 Paris (2002).

[5] H. Burkhardt et al, "Observation of a Fast Single-Bunch Transverse Instability on Protons in the SPS," EPAC 2004 Lucerne (2004).

[6] E. Metral et al, "The Fast Vertical Single-Bunch Instability after Injection into the CERN Super Proton Synchrotron," EPAC 2006 Edinburgh (2006).

[7] Y.H. Chin, "Transverse Mode Coupling Instability in a Double RF System, " Part. Acc. 45: 209, CERN-SL-93-03-AP (1993).

[8] E. Metral, "The SPS Impedance Budget," CERN SPS Upgrade Meeting, 21.08.2007.

[9] E. Shaposhnikova, "Studies of Beam Behavior in Double RF System," CERN APC 06.06.2007.

[10] J.-P. Delahaye et al, "Shaping of Proton Distribution for Raising the Space Charge of the CERN PS Booster," 11th HEACC, Geneva, 1980

[11] A. Blas, S. Hancock, M. Lindroos, S. Koscielniak, "Hollow Bunch Distributions at High Intensity in the PS Booster," EPAC 2000, Vienna (2000).

[12] R. Garoby, S. Hancock, "New Techniques for Tailoring Longitudinal Density in a Proton Synchrotron," EPAC 94, London (1994).

[13] C. Carli, "Creation of Hollow Bunches using a Double Harmonic RF System", CERN/PS 2001-073 (AE) (2001).

[14] C. Carli and M. Chanel, "New Methods to Create Hollow Bunches," Proc. HB2002, Batavia, AIP CP642, CERN-PS-2002-035-AE (2002)

[15] J. Wei, "IBS Theories, Codes, and Benchmarking", IBS'07 workshop, Daresbury (2007).

[16] E. Shaposhnikova et al, "Beam Transfer Functions and Beam Stabilisation in a Double RF System," PAC2005 Knoxville

[17] E. Shaposhnikova, "Bunched Beam Transfer Matrices in Single and Double RF systems," CERN SL/94-19-RF (1994).

[18] G. Rumolo, F. Zimmermann, "Practical User Guide for HEADTAIL," CERN SL-Note-2002-036-AP (2002).

[19] G. Rumolo, private communication, 07.08.2007

[20] F. Ruggiero, S. Berg, "Stability Diagrams for Landau Damping," PAC'97 Vancouver (1997)

[21] M.A. Furman, "E-Cloud in PS2, PS+, SPS+," Proceedings LHC-LUMI-06, CERN-2007-002, CARE-Conf-07-004-HHH (2007).

[22] P.W. Krempel, "The Abel-Type Integral Transformation and Its Application to Density Distributions of Particle Beams," MPS/Int.BR/74-1 (1974).

[23] I. Santiago Gonzalez, "Loss of Longitudinal Landau Damping in the LHC Injectors," CERN-AB-Note-2008-001, CARE-NOTE-2007-012-HHH (2007).

[24] F.J. Sacherer, "A Longitudinal Stability Criterion for Bunched Beams," CERN/MPS/BR 73-1, IEEE Tr. NS 20, 3, 825 (1973).

[25] E. Metral, "Longitudinal Bunched Beam Coherent Modes: From Stability to Instability and Inversely," CERN-AB-2004-002 (ABP).

[26] K.Y. Ng, "Comments on Landau Damping due to Synchrotron Frequency Spread," FERMILAB-FN-0762-AD (2005).

[27] S. Koscielniak, "Transfer Functions of Hollow Bunches," TRI-DN-99-25 (1999).

[28] E. Shaposhnikova, "Longitudinal Phenomena during the LHC Cycle," Chamonix XI, CERN-SL-2001-003 DI (2001).

[29] E. Shaposhnikova, “Longitudinal Stability of the LHC Beam in the SPS,” CERN SL-Note-2001-035-HRF, 2001.

[30] J. Wei, “IBS Theories, Codes, and Benchmarking,” IBS07 workshop, Daresbury (2007).

[31] Information on the BBFP code can be found in the CARE-HHH code web repository; see *http://oraweb.cern.ch:9000/pls/hhh/code_website.disp_allcat*. The code is available from the author.